WNT/RYK signaling functions as an antiinflammatory modulator in the lung mesenchyme

Hyun-Taek Kim[a,b,c,d,e,1], Paolo Panza[a,b,c], Khrievono Kikhi[f], Yuko Nakamichi[g], Ann Atzberger[f], Stefan Guenther[b,h], Clemens Ruppert[c,i], Andreas Guenther[b,c,i], and Didier Y. R. Stainier[a,b,c,1]

A number of inflammatory lung diseases, including chronic obstructive pulmonary disease, idiopathic pulmonary fibrosis, and pneumonia, are modulated by WNT/β-catenin signaling. However, the underlying molecular mechanisms remain unclear. Here, starting with a forward genetic screen in mouse, we identify the WNT coreceptor Related to receptor tyrosine kinase (RYK) acting in mesenchymal tissues as a cell survival and antiinflammatory modulator. *Ryk* mutant mice exhibit lung hypoplasia and inflammation as well as alveolar simplification due to defective secondary septation, and deletion of *Ryk* specifically in mesenchymal cells also leads to these phenotypes. By analyzing the transcriptome of wild-type and mutant lungs, we observed the up-regulation of proapoptotic and inflammatory genes whose expression can be repressed by WNT/RYK signaling in vitro. Moreover, mesenchymal *Ryk* deletion at postnatal and adult stages can also lead to lung inflammation, thus indicating a continued role for WNT/RYK signaling in homeostasis. Our results indicate that RYK signaling through β-catenin and Nuclear Factor kappa B (NF-κB) is part of a safeguard mechanism against mesenchymal cell death, excessive inflammatory cytokine production, and inflammatory cell recruitment and accumulation. Notably, RYK expression is down-regulated in the stromal cells of pneumonitis patient lungs. Altogether, our data reveal that RYK signaling plays critical roles as an antiinflammatory modulator during lung development and homeostasis and provide an animal model to further investigate the etiology of, and therapeutic approaches to, inflammatory lung diseases.

WNT/RYK signaling | lung mesenchyme | inflammatory lung disease

Significance

WNT/β-catenin signaling is critical for lung development, and homeostasis and it has also been implicated in inflammatory lung diseases. However, the underlying molecular mechanisms, especially those at play during inflammatory conditions, are unclear. Here, we show that loss of the WNT coreceptor Related to receptor tyrosine kinase (RYK) specifically in mesenchymal cells results in lung inflammation. Our data indicate that RYK signaling through β-catenin and Nuclear Factor kappa B (NF-κB) is part of a safeguard mechanism against mesenchymal cell death, excessive inflammatory cytokine production, and inflammatory cell recruitment and accumulation.

During inflammatory lung diseases, lung mesenchymal cells play a crucial role in the inflammatory process and also contribute to tissue remodeling. Lung mesenchymal cells, including airway smooth muscle cells and fibroblasts, can produce and secrete a variety of inflammatory cytokines and chemokines, cell adhesion molecules, as well as extracellular matrix proteins, which lead to inflammatory cell recruitment and activation (1, 2). Occasionally, the inflammatory response in the lung is associated with structural cells undergoing apoptotic cell death (3, 4). In addition, apoptotic cells also secrete inflammatory cytokines and can recruit immune cells (5–7). A delicate balance of immune cell recruitment and apoptosis is required for lung homeostasis; however, the molecular mechanisms underlying mesenchymal–immune cell cross-talk are not fully understood.

Many components of the WNT signaling cascade are expressed in lung mesenchymal tissues during development and homeostasis. For instance, *WNT-2, FZD-1, -4,* and *-7* as well as *LEF1* are expressed selectively in mesenchymal cells (8–10). Moreover, dysregulated WNT/β-catenin signaling contributes to the pathogenesis of inflammatory lung diseases, including chronic obstructive pulmonary disease (COPD), idiopathic pulmonary fibrosis (IPF), and asthma (10, 11). However, the precise role of WNT/β-catenin signaling during lung inflammation remains unclear.

Related to receptor tyrosine kinase (RYK) functions as a WNT coreceptor and belongs to the atypical receptor tyrosine kinase family (12, 13). In a previous study, we reported that RYK is strongly expressed in airway epithelial cells and moderately expressed in lung alveolar epithelial and mesenchymal cells. *Ryk* knockout (KO) and SL (stop loss) mice exhibit a combination of goblet cell hyperplasia and inflammation, and this latter phenotype is not observed in mice lacking *Ryk* function in epithelial cells (14). A few studies have focused on tissue- or cell type–specific functions of RYK. For example, WNT/RYK participates in motor cortex remapping after spinal cord injury and in neuropil formation in the outer retina (15, 16). An in vitro study showed that WNT-5A/RYK signaling in endothelial cells controls vascular permeability through cytoskeleton remodeling (17). However, the role of RYK in mesenchymal tissues has not yet been studied.

Here we reveal a role for RYK in mesenchymal cell survival and the inflammatory response during lung development and homeostasis. Our results from in vivo and

in vitro manipulations suggest that alterations of WNT/RYK signaling through NF-κB contribute to the pathogenesis of inflammatory lung diseases. Two different mesenchymal *Ryk* deletion models display extensive inflammation at developmental and adult stages, thereby providing a useful platform to further investigate the etiology and treatment of inflammatory lung diseases.

Results

***Ryk* Mutant Mice Exhibit Lung Inflammation and Alveolar Simplification.** In a previous study, we reported the identification and analysis of a SL mutant allele of *Ryk*, which leads to lung hypoplasia and inflammation (Fig. 1 *A* and *B*) (14). Epithelial-specific deletion of *Ryk* leads to goblet cell hyperplasia and mucus hypersecretion without lung inflammation (14). Here, we focus on the inflammation phenotype. To determine which immune cell types accumulate in $Ryk^{SL/SL}$ lungs, we performed histological analyses and immunostaining. At the histological level, $Ryk^{SL/SL}$ lungs display infiltration of macrophages and monocytes, neutrophils, and also lymphocytes (*SI Appendix,* Fig. S1*A*). The number of both alveolar and interstitial macrophages was markedly increased in $Ryk^{SL/SL}$ lungs at postnatal day 7 (P7) (Fig. 1*C*). In addition, immunostaining analyses revealed increased numbers in P7 $Ryk^{SL/SL}$ lungs of hematopoietic cells (CD45$^+$) (Fig. 1*D*), including lymphocytes (CD3$^+$ and CD19$^+$) and macrophages (MAC2$^+$) (*SI Appendix,* Fig. S1 *B–D*). We next investigated the stage at which an accumulation

of inflammatory cells is first observed in $Ryk^{SL/SL}$ lungs. While $Ryk^{SL/SL}$ lungs were partially collapsed at P0, inflammatory cells were first recruited in mutant lungs starting around P1 (*SI Appendix,* Fig. S1 *E* and *F*), indicating that the loss of *Ryk* function causes the recruitment of inflammatory cells into the lung starting at postnatal stages. Moreover, many immune cells were proliferating in $Ryk^{SL/SL}$ lungs (*SI Appendix,* Fig. S2 *A* and *B*), indicating that the marked increase in the number of inflammatory cells is due to both recruitment from other tissues and local proliferation. We next performed α-smooth muscle actin (α-SMA) and elastin (ELN) immunostaining to visualize secondary septa in P7 lungs. $Ryk^{SL/SL}$ mice exhibited severe defects in secondary septa formation and a significant reduction in α-SMA and ELN expression at P7 (Fig. 1 *E* and *F*), suggesting that RYK participates in myofibroblast development or maintenance and, consequently, secondary septa formation during lung maturation.

Loss of vascular integrity in inflammatory conditions can trigger immune cell infiltration into the lung parenchyma and alveolar spaces (18). To evaluate vessel integrity in $Ryk^{SL/SL}$ lungs, we injected Evans blue dye intracardially at P3. While Evans blue dye was retained in the blood vessels of wild-type (WT) lungs, it diffused into the $Ryk^{SL/SL}$ lung parenchyma (Fig. 1*G*). In addition, the postnatal expression of platelet endothelial cell adhesion molecule-1 (PECAM-1), an adhesion molecule that contributes to the maintenance of vascular integrity (19), appeared to be reduced in $Ryk^{SL/SL}$ lungs compared with $Ryk^{+/+}$ siblings, and its localization at endothelial cell junction also appeared more punctate (Fig. 1*H* and *SI Appendix,* Fig. S2*C*). These data indicate
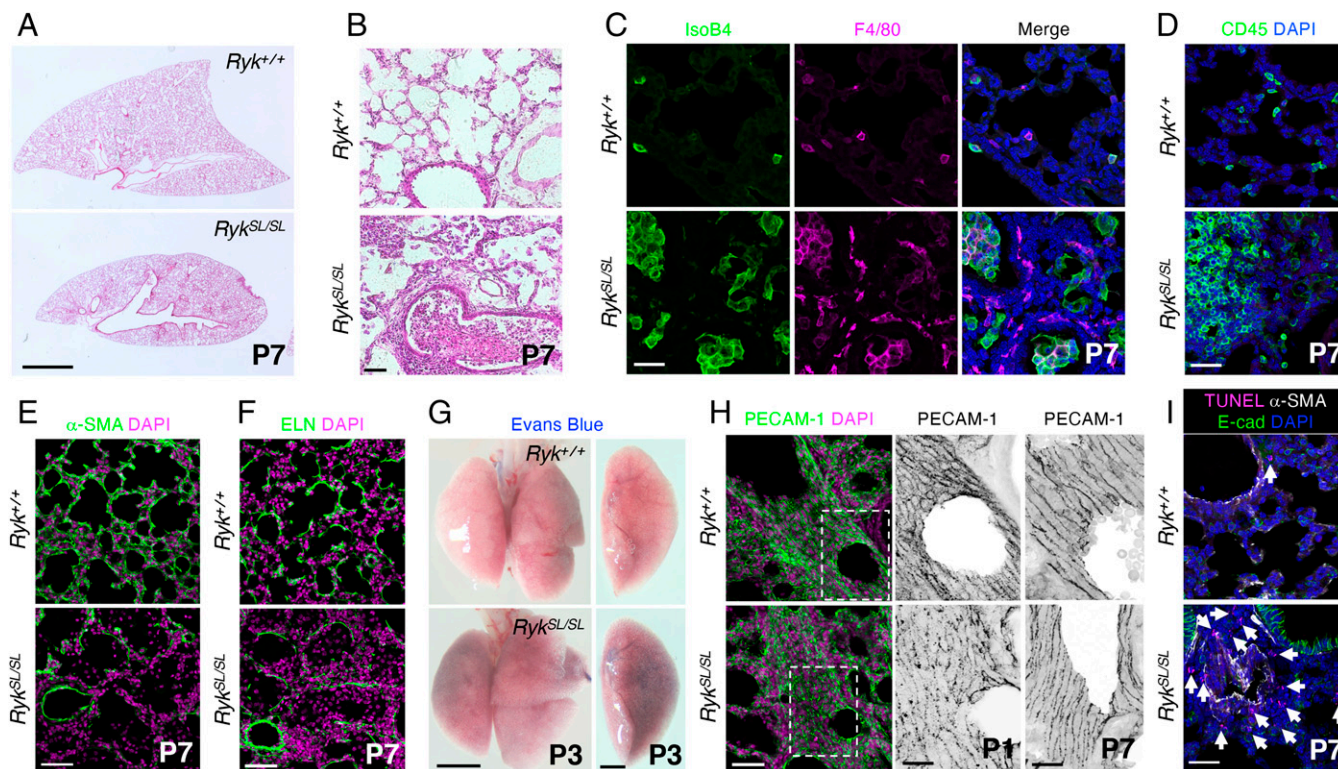

Fig. 1. *Ryk* deficiency leads to lung hypoplasia and inflammation. (*A*) Hematoxylin and eosin (H&E) staining of P7 $Ryk^{+/+}$ (*n* = 10) and $Ryk^{SL/SL}$ (*n* = 12) lung sections. (*B*) High magnification of H&E-stained P7 $Ryk^{+/+}$ (*n* = 10) and $Ryk^{SL/SL}$ (*n* = 12) lung sections. (*C*) IsoB4 staining (immune cells) and F4/80 immunostaining (alveolar and interstitial macrophages) in P7 $Ryk^{+/+}$ (*n* = 10) and $Ryk^{SL/SL}$ (*n* = 12) lung sections. (*D*) Immunostaining for CD45 (hematopoietic cells) in P7 $Ryk^{+/+}$ (*n* = 10) and $Ryk^{SL/SL}$ (*n* = 12) lung sections. (*E*) Immunostaining for α-SMA (to mark myofibroblasts) in P7 $Ryk^{+/+}$ (*n* = 10) and $Ryk^{SL/SL}$ (*n* = 12) lung sections. (*F*) Immunostaining for ELN (to mark secondary septa) in P7 $Ryk^{+/+}$ (*n* = 10) and $Ryk^{SL/SL}$ (*n* = 12) lung sections. (*G*) Representative images of P3 $Ryk^{+/+}$ (*n* = 6) and $Ryk^{SL/SL}$ (*n* = 6) lungs injected with Evans blue dye. (*H*) Immunostaining for PECAM-1 (endothelial cells) in P1 and P7 $Ryk^{+/+}$ (*n* = 5) and $Ryk^{SL/SL}$ (*n* = 5) lung sections. High-magnification image of the areas in the dashed boxes is shown in the *Middle* panels. (*I*) TUNEL staining and immunostaining for α-SMA and E-cadherin in P7 $Ryk^{+/+}$ (*n* = 10) and $Ryk^{SL/SL}$ (*n* = 12) lung sections. Arrows point to TUNEL-positive cells. (Scale bars: 2 mm for *A* and *G*, *Left*, 1 mm for *G*, *Right*; 50 μm for *B*, *E*, *F*, and *H*, *Left*; and 30 μm for *C*, *D*, *H*, *Right*, and *I*.)

that *Ryk* deficiency leads to defects in lung vessel wall integrity as well as increased permeability at postnatal stages.

Since cell death can induce endothelial barrier dysfunction and inflammatory cell recruitment (3, 5), we examined cell death in *Ryk^{SL/SL}* lungs using terminal deoxynucleotidyl transferase dUTP nick end labeling (TUNEL) staining. The number of dead cells was significantly increased in *Ryk^{SL/SL}* lungs at postnatal stages but not at embryonic day 18.5 (E18.5) (Fig. 1*I* and *SI Appendix,* Fig. S2*D*). Moreover, most dead cells were observed in the mesenchymal compartment surrounding blood vessels (Fig. 1*I* and *SI Appendix,* Fig. S2*D*), indicating that RYK is required for the survival of mesenchymal cells in the postnatal lung. Notably, *Ryk^{SL/SL}* mice exhibited no obvious defects in other organs, including the heart, kidney, and liver (*SI Appendix,* Fig. S2*E*). Overall, these data indicate that in the postnatal lung, loss of *Ryk* function leads to cell death in the mesenchyme and triggers inflammatory cell recruitment and local proliferation.

Mesenchymal *Ryk* Deletion Leads to Lung Inflammation and Alveolar Simplification. To investigate the cell type–specific functions of *Ryk* during mouse lung development, we deleted the gene in mesenchymal cells using a *Dermo1/Twist2-Cre* line (hereafter *Dermo1-Cre⁻-Ryk^{fl/+}* or *Dermo1-Ryk^{WT}* and *Dermo1-Cre⁺-Ryk^{fl/fl}* or *Dermo1-Ryk^{cKO}*) and obtained specific loss of *Ryk* expression in lung mesenchymal cells (*SI Appendix,* Fig. S3*A*). Similar to *Ryk* KO and SL mice (14, 20), *Dermo1-Ryk^{cKO}* mice exhibited growth retardation and hypoplastic lungs at P7 (Fig. 2 *A–C*) and subsequently died around P14. In addition, *Dermo1-Ryk^{cKO}* lungs displayed inflammatory cell accumulation and alveolar simplification at P7 (*SI Appendix,* Fig. S3 *B–D*). The inflammatory cells observed in *Dermo1-Ryk^{cKO}* lungs included macrophages, monocytes, neutrophils, and lymphocytes, as judged by cell morphology and marker analysis (Fig. 2*D* and *SI Appendix,* Fig. S3*E*). To quantitatively characterize the various inflammatory cell populations, we performed immunophenotyping using flow cytometry (*SI Appendix,* Fig. S3*F*). The number of immune cells (CD45⁺) was markedly increased in *Dermo1-Ryk^{cKO}* lungs compared with *Dermo1-Ryk^{WT}* lungs (Fig. 2 *D* and *E*). *Dermo1-Ryk^{cKO}* lungs exhibited increased numbers of eosinophils (CD11c⁻ SiglecF⁺), dendritic cells (CD11C⁺ SiglecF⁻), and neutrophils (CD11b^{hi} Ly6G^{hi}) (Fig. 2*E*). In addition, the number of macrophages (CD11c^{hi}
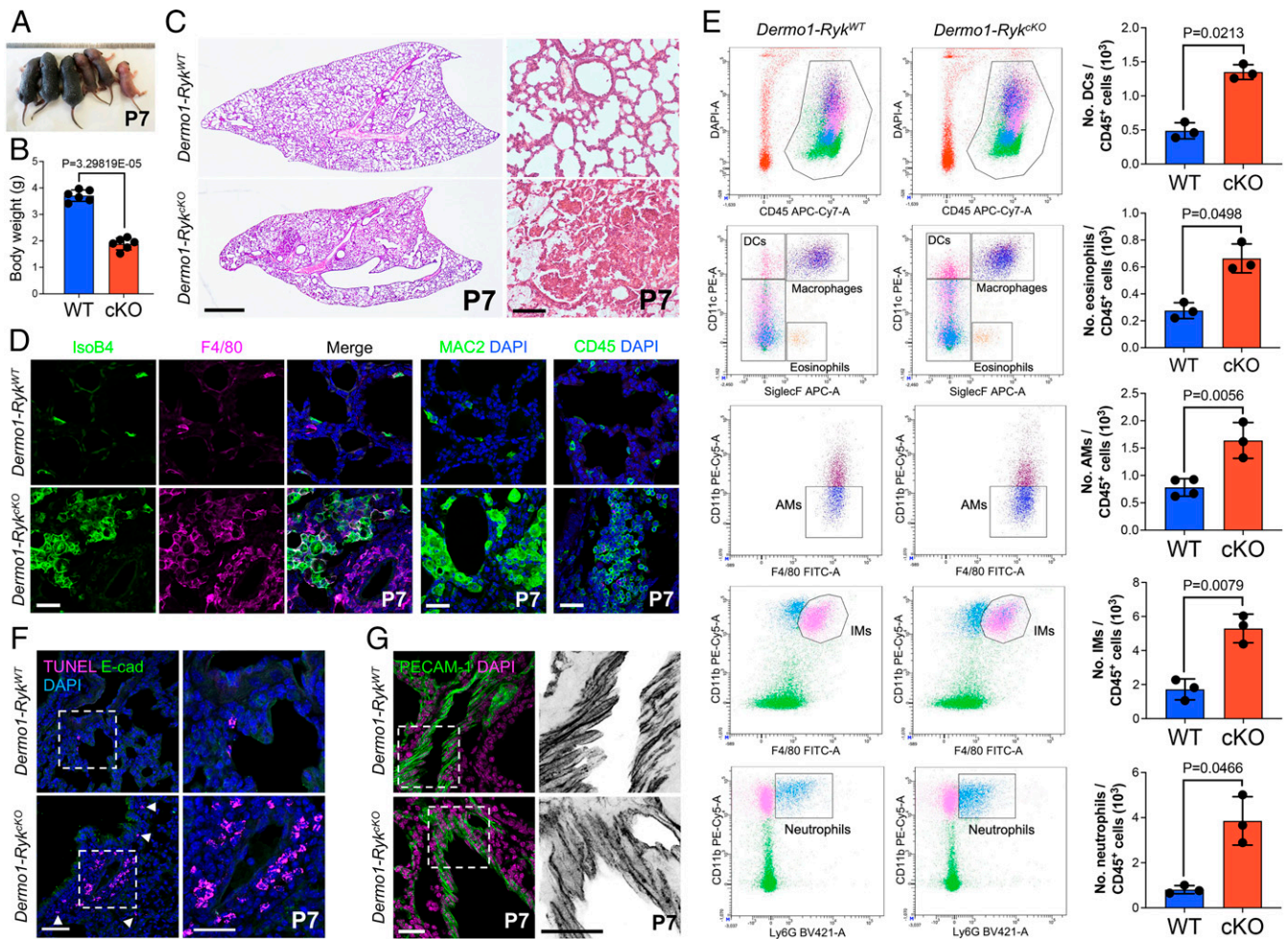

Fig. 2. Mesenchymal *Ryk* deletion leads to lung inflammation. (*A*) General appearance of P7 *Dermo1-Ryk^{WT}* (*n* = 3) and *Dermo1-Ryk^{cKO}* (*n* = 3) mice. (*B*) Body weight of P7 *Dermo1-Ryk^{WT}* (*n* = 6) and *Dermo1-Ryk^{cKO}* (*n* = 5) mice. (*C*) H&E staining of P7 *Dermo1-Ryk^{WT}* (*n* = 10) and *Dermo1-Ryk^{cKO}* (*n* = 9) lung sections. (*D*) IsoB4 staining (immune cells) and immunostaining for F4/80 (alveolar and interstitial macrophages), MAC2 (alveolar and interstitial macrophages), and CD45 (hematopoietic cells) of P7 *Dermo1-Ryk^{WT}* (*n* = 10) and Dermo1-Ryk^{cKO}* (*n* = 9) lung sections. (*E*) Representative flow cytometry analysis of CD45⁺ hematopoietic cells from the lungs of P3 *Dermo1-Ryk^{WT}* (*n* = 3) and *Dermo1-Ryk^{cKO}* (*n* = 4) mice. Bar graphs representing the number of alveolar macrophages (AMs), dendritic cells (DCs), eosinophils, interstitial macrophages (IMs), and neutrophils as measured by flow cytometry in the lungs of P3 *Dermo1-Ryk^{WT}* (*n* = 3) and *Dermo1-Ryk^{cKO}* (*n* = 4) mice. (*F*) TUNEL staining and E-cadherin immunostaining of P7 *Dermo1-Ryk^{WT}* (*n* = 10) and *Dermo1-Ryk^{cKO}* (*n* = 9) lung sections. High-magnification image of the areas in the dashed boxes is shown on the *Right*. Arrowheads point to TUNEL-positive cells. (*G*) Immunostaining for PECAM-1 of P7 *Dermo1-Ryk^{WT}* (*n* = 10) and *Dermo1-Ryk^{cKO}* (*n* = 9) lung sections. High-magnification image of the areas in the dashed boxes is shown on the *Right*. Error bars are means ± SEM, two-tailed Student's *t* test. (Scale bars: 1 mm for *C, Left*; 100 μm for *C, Right*; 50 μm for *F, Left*; and 30 μm for *D, F, Right*, and *G*.)

SiglecF^{hi}), including alveolar macrophages (CD11b^− F4/80^{hi}) and interstitial macrophages (CD11b^{hi} F4/80^{hi}), was significantly increased in *Dermo1-Ryk^{cKO}* lungs (Fig. 2*E*). These data indicate that *Ryk* deficiency in the mesenchyme leads to an increase of both resident and circulating immune cells in the lung. We next examined cell death in *Dermo1-Ryk^{cKO}* lungs using TUNEL staining. Similar to our observations in *Ryk* SL mice, the number of dead cells was greatly increased in the perivascular mesenchyme of P7 *Dermo1-Ryk^{cKO}* lungs (Fig. 2*F*). This increase in cell death in *Dermo1-Ryk^{cKO}* lungs was apparent starting at around P1 (*SI Appendix*, Fig. S4*A*). In addition, we observed defects in vessel integrity in *Dermo1-Ryk^{cKO}* lungs at P3 and P7 but not at P0 (Fig. 2*G* and *SI Appendix*, Fig. S4 *B and C*), indicating that mesenchymal cell death causes vessel integrity defects in *Dermo1-Ryk^{cKO}* lungs. However, using *Shh-Cre*, *Tek-CreER^{T2}*, and *Lyz2-Cre* lines, epithelial-, endothelial-, or myeloid lineage–specific *Ryk* deletion caused no obvious inflammatory cell recruitment and accumulation into the lungs (14) (*SI Appendix*, Fig. S5 *A–E*). Overall, these data indicate that in the lung mesenchyme, RYK functions as a survival factor and/or immunomodulator starting at early postnatal stages.

RYK Signaling Inhibits Apoptosis-Associated Gene Expression and Restricts the Immune Response. To identify mesenchymal genes regulated by *Ryk* function that are involved in postnatal lung development, we performed transcriptomic analysis of P0 *Dermo1-Ryk^{WT}* and *Dermo1-Ryk^{cKO}* lungs. From gene ontology (GO) analysis, the up-regulated genes were mostly associated with immune response and apoptosis, and the down-regulated genes with WNT signaling (Fig. 3*A* and *SI Appendix*, Fig. S6*A* and Dataset S1). We focused on the up-regulated genes and first validated their expression by qPCR. The expression of immune response genes, including *Bcl3*, *Ccl2*, *Il1f9*, *Il1r2*, and *Serpina3f*, was significantly up-regulated in *Dermo1-Ryk^{cKO}* lungs starting at P1 (Fig. 3*B* and *SI Appendix*, Fig. S6*B*). In addition, the expression of apoptosis genes, including *Casp4*, *Fas*, *Ddit4*, *Pim1*, and *Gadd45g*, was significantly up-regulated already at P0 in *Dermo1-Ryk^{cKO}* lungs compared with wild type (Fig. 3*C* and *SI Appendix*, Fig. S6*C*).

We next examined the expression of *Ccl2*/CCL2 and *Bcl3*/BCL3 by qPCR, in situ hybridization, and Western blotting or immunostaining. The expression of *Ccl2* was strongly up-regulated and that of *Bcl3* moderately up-regulated in P2
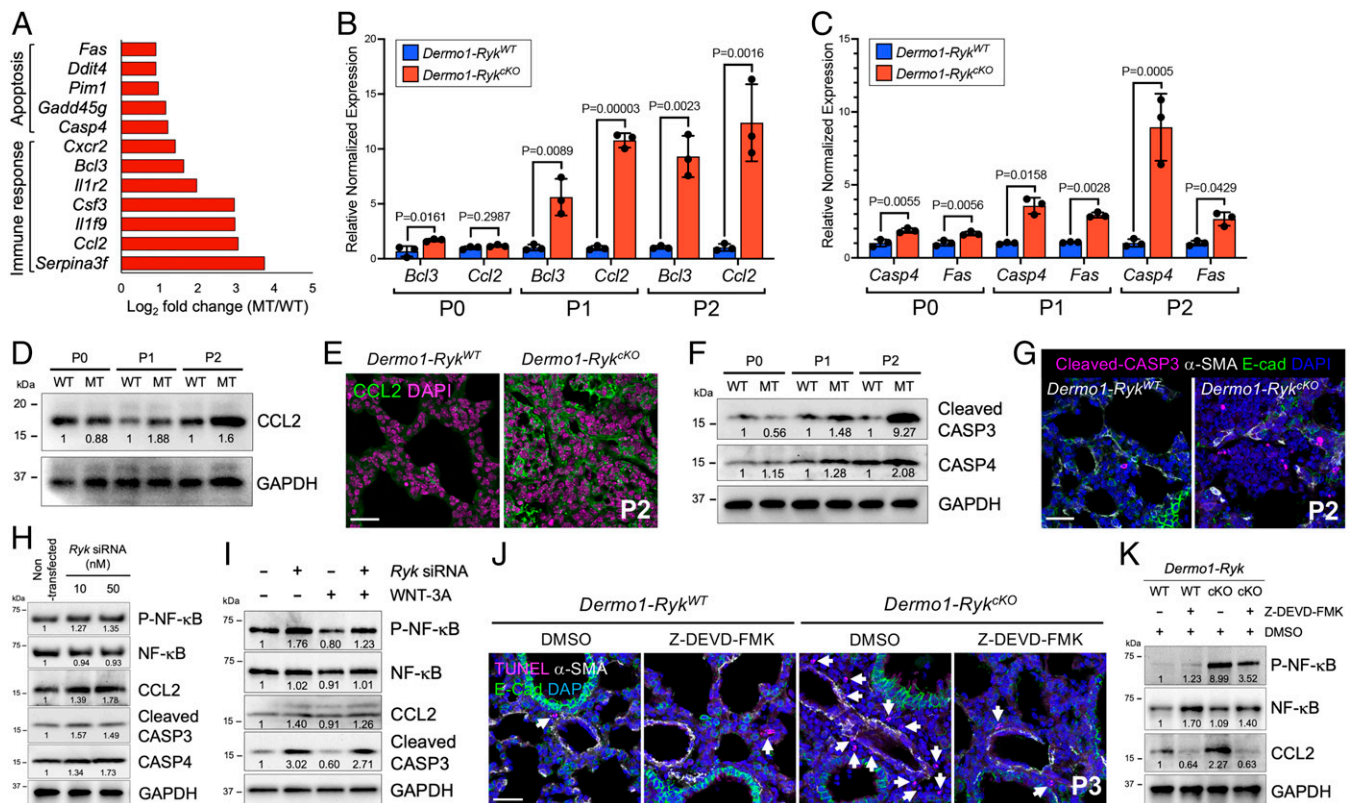

Fig. 3. RYK inhibits cell death in the lung mesenchyme. (*A*) RNA-sequencing fold change (log$_2$) of differentially expressed genes in P0 *Dermo1-Ryk^{WT}* (*n* = 3) compared with *Dermo1-Ryk^{cKO}* (*n* = 3) lungs. (*B*) qPCR analysis of *Bcl3* and *Ccl2* mRNA levels in P0, P1, and P2 *Dermo1-Ryk^{WT}* and *Dermo1-Ryk^{cKO}* lungs. (*C*) qPCR analysis of *Casp4* and *Fas* mRNA levels in P0, P1, and P2 *Dermo1-Ryk^{WT}* and *Dermo1-Ryk^{cKO}* lungs. (*D*) Representative Western blot (from three individual sets of lung lysates) for CCL2 in P0, P1, and P2 *Dermo1-Ryk^{WT}* and *Dermo1-Ryk^{cKO}* lungs. GAPDH, glyceraldehyde-3-phosphate dehydrogenase. Values represent the densitometric ratio after normalization to GAPDH. (*E*) Immunostaining for CCL2 in P2 *Dermo1-Ryk^{WT}* (*n* = 6) and *Dermo1-Ryk^{cKO}* (*n* = 6) lung sections. (*F*) Representative Western blot (from three individual sets of lung lysates) for cleaved CASP3 and CASP4 in P0, P1, and P2 *Dermo1-Ryk^{WT}* and *Dermo1-Ryk^{cKO}* lungs. Values represent the densitometric ratio after normalization to GAPDH. (*G*) Immunostaining for cleaved CASP3, α-SMA, and E-cadherin in P2 *Dermo1-Ryk^{WT}* (*n* = 6) and *Dermo1-Ryk^{cKO}* (*n* = 6) lung sections. (*H*) Representative Western blot (from three individual sets of cell lysates) for NF-κB, phospho–NF-κB, CCL2, cleaved CASP3, and CASP4 in nontransfected and *Ryk* siRNA (10 nM or 50 nM)-transfected NIH 3T3 fibroblasts. Values represent densitometric ratios after normalization to GAPDH, except for phospho–NF-κB, which was normalized to GAPDH and total NF-κB. (*I*) Representative Western blot (from three individual sets of cell lysates) for NF-κB, phospho–NF-κB, CCL2, and cleaved CASP3 upon stimulation with WNT-3A and/or cotransfection of *Ryk* siRNA in NIH 3T3 fibroblasts. Values represent densitometric ratios after normalization to GAPDH, except for phospho–NF-κB, which was normalized to GAPDH and total NF-κB. (*J*) TUNEL staining and immunostaining for α-SMA (to mark smooth muscle) and E-cadherin in DMSO- or Z-DEVD-FMK–treated P3 *Dermo1-Ryk^{WT}* (*n* = 6) and *Dermo1-Ryk^{cKO}* (*n* = 6) lung sections. Arrows point to TUNEL-positive cells. (*K*) Representative Western blot (from three individual sets of lung lysates) for NF-κB, phospho–NF-κB, and CCL2 in DMSO- or Z-DEVD-FMK–treated P3 *Dermo1-Ryk^{WT}* and *Dermo1-Ryk^{cKO}* lungs. Values represent densitometric ratios after normalization to GAPDH, except for phospho–NF-κB, which was normalized to GAPDH and total NF-κB. Error bars are means ± SEM, two-tailed Student's *t* test. Ct values are listed in *SI Appendix*, Table S2. (Scale bars: 50 μm for *G* and 30 μm for *E* and *J*.)

Dermo1-Ryk^{cKO} lungs (*SI Appendix*, Fig. S6 *D and E*). CCL2 expression was also increased in mesenchymal cells and immune cells in P2 *Dermo1-Ryk^{cKO}* lungs (Fig. 3 *D and E* and *SI Appendix*, Fig. S7 *A–C*), indicating that RYK can repress *Ccl2* expression in the lung mesenchyme at postnatal stages. We also examined the expression of the apoptosis genes *Casp4* and *Fas* in developing lungs. *Casp4* and *Fas* expression was significantly increased in mesenchymal cells of P2 *Dermo1-Ryk^{cKO}* (*SI Appendix*, Fig. S6 *D and F*). Protein levels of CASP4 and cleaved CASP3, the latter a hallmark of active apoptosis (21), were significantly increased in *Dermo1-Ryk^{cKO}* lungs starting at P1, and even more strongly at P2 (Fig. 3 *F and G*). These data indicate that loss of *Ryk* function in lung mesenchymal cells can cause their death, and that subsequently the dying cells induce the expression of cytokines.

To test whether *Ryk* deficiency also leads to the upregulation of downstream genes in vitro, we performed *Ryk* knockdown in NIH3T3 mouse embryonic fibroblasts (*SI Appendix*, Fig. S7*D*). Since NF-κB signaling is a master regulator of the inflammatory response (22, 23), we first examined the activation status of NF-κB in *Ryk* knockdown cells. *Ryk* knockdown led to increased phosphorylation of NF-κB and IκKαβ (a positive regulator of NF-κB signaling that is activated by phosphorylation), as well as IκBα (a negative regulator of NF-κB signaling that is inactivated by phosphorylation) (Fig. 3*H* and *SI Appendix*, Fig. S7 *E and F*). In addition, expression of CCL2, cleaved CASP3, and CASP4 was also increased when *Ryk* was knocked down in NIH 3T3 cells (Fig. 3*H*). As RYK is known to modulate both β-catenin–dependent and –independent signaling (12, 13), we examined whether RYK participates in WNT/β-catenin signaling by testing GSK-3β–induced phosphorylation of CTNNB1/β-catenin. *Ryk* knockdown led to increased phosphorylation of CTNNB1 (*SI Appendix*, Fig. S7*G*) and could prevent the activation of WNT/β-catenin by WNT-3A, but it had no effect on the blockade of this pathway by WNT-5A (*SI Appendix*, Fig. S7*H*). These data indicate that RYK participates in β-catenin–dependent signaling in fibroblasts. WNT-3A treatment alone led to a reduction in NF-κB phosphorylation and lower levels of cleaved CASP3 in fibroblasts (Fig. 3*I*). Conversely, *Ryk* knockdown in combination with WNT-3A treatment led to an increase in NF-κB phosphorylation and CCL2 expression as well as cleaved CASP3 levels, reverting the effect of WNT/β-catenin activation (Fig. 3*I*). In summary, RYK participates in the WNT/β-catenin signaling pathway, and it can repress the expression of proinflammatory and proapoptotic mediators/factors in fibroblasts.

To examine whether Caspase inactivation could ameliorate the lung phenotype in *Dermo1-Ryk^{cKO}* mice, we used a broad-spectrum Caspase inhibitor (Benzyloxycarbonyl-Val-Ala-Asp(OMe)-fluoromethylketone, Z-VAD-FMK) as well as a Caspase-3 inhibitor (Benzyloxycarbonyl-Asp(OMe)-Glu(OMe)-Val-Asp(OMe)-fluoromethylketone, Z-DEVD-FMK) in vivo. These compounds were injected intraperitoneally into lactating mothers at P0, P1, and P2, and the lungs were collected at P3. Dimethyl sulfoxide (DMSO)-treated *Dermo1-Ryk^{cKO}* mice exhibited severe lung inflammation at P3 (*SI Appendix*, Fig. S8 *A–C*). Conversely, the lung phenotypes of *Dermo1-Ryk^{cKO}* mice were partially rescued by treatment with the Caspase inhibitors (*SI Appendix*, Fig. S8 *A–C*). Whereas a high number of dying cells was observed in *Dermo1-Ryk^{cKO}* lungs, this number was significantly decreased in Caspase inhibitor–treated *Dermo1-Ryk^{cKO}* lungs (Fig. 3*J* and *SI Appendix*, Fig. S8*D*). In addition, the levels of NF-κB phosphorylation and CCL2 expression were also reduced in Caspase inhibitor–treated *Dermo1-Ryk^{cKO}* lungs compared with control (Fig. 3*K* and *SI Appendix*, Fig. S8*E*). These data indicate that in

Ryk-deficient conditions, cell death leads to lung inflammation. Altogether, these data suggest that WNT/RYK signaling has an antiapoptotic and/or antiinflammatory role in fibroblasts and developing lung mesenchymal cells.

RYK Participates in Lung Maturation and Homeostasis. Since lung inflammation and cell death in *Ryk*-deficient mice were observed specifically at postnatal stages, we also investigated *Ryk* function in the mesenchyme during lung maturation and homeostasis. When we deleted *Ryk* in mesenchymal cells by injecting tamoxifen between P0 and P2 in *Gli1-CreER^{T2}*;*Ryk*-floxed mice (hereafter *Gli1-CreER^{T2}-Ryk^{fl/fl}* or *Gli1-Ryk^{WT}* and *Gli1-CreER^{T2+}-Ryk^{fl/fl}* or *Gli1-Ryk^{cKO}*), we found no obvious growth retardation or lung hypoplasia at P10 (Fig. 4 *A and B*), unlike what we observed in *Ryk* SL and *Dermo1-Ryk^{cKO}* mice. Instead, these *Gli1-Ryk^{cKO}* mice exhibited inflammatory cell accumulation in the lungs (Fig. 4*C* and *SI Appendix*, Fig. S9*A*). At P10, most inflammatory cells in *Gli1-Ryk^{cKO}* mice were macrophages (IsoB4, F4/80, and MAC2$^+$) and lymphocytes (CD45$^+$) (Fig. 4 *D and E* and *SI Appendix*, Fig. S9 *A and B*). In addition, an increased number of dead cells was observed in the mesenchymal cells surrounding the blood vessels of P10 *Gli1-Ryk^{cKO}* lungs (Fig. 4*F*). *Gli1-Ryk^{cKO}* mice also exhibited vessel integrity defects, as revealed by the lower expression of PECAM-1 in the lungs and diffusion of Evans blue dye into the lung parenchyma (Fig. 4*G* and *SI Appendix*, Fig. S9*C*). These data suggest that RYK also has a crucial function in preventing mesenchymal cell death and excessive inflammatory cell recruitment during lung maturation. To determine whether RYK participates in lung homeostasis, we deleted *Ryk* at adult stages by employing a *Rosa26-CreER^{T2}* driver line (hereafter *Rosa26-CreER^{T2}-Ryk^{fl/fl}* or *Rosa26-Ryk^{WT}* and *Rosa26-CreER^{T2+}-Ryk^{fl/fl}* or *Rosa26-Ryk^{cKO}*) (*SI Appendix*, Fig. S9*D*). Inflammatory cells accumulated in the lungs of *Rosa26-Ryk^{cKO}* mice at adult stages (*SI Appendix*, Fig. S9 *E and F*), suggesting that RYK functions as an antiinflammatory modulator in the lung during homeostasis as well. Next, we selectively deleted *Ryk* in mesenchymal cells at adult stages using the *Gli1-CreER^{T2}* line (*SI Appendix*, Fig. S9*G*). *Gli1-Ryk^{cKO}* lungs exhibited inflammatory cell accumulation and disrupted alveolar structure, as well as an increased number of dead cells (*SI Appendix*, Fig. S9 *H–J*), indicating that *Ryk* deficiency in mesenchymal cells is sufficient for inflammatory cell recruitment during lung homeostasis. Overall, RYK functions in the mesenchyme to promote cell survival and restrict the immune response during lung maturation and homeostasis.

RYK Is Down-Regulated in Patients with Pneumonitis. Since WNT/β-catenin signaling plays antiinflammatory roles during inflammatory lung diseases in mice and humans (24, 25), we tested RYK expression in the lungs of five healthy controls and 10 pneumonitis patients. Similar to our previous findings (14), in the lungs of healthy controls, high levels of RYK were detected in the airway epithelium and moderate levels in immune cells and stromal cells (Fig. 4*H* and *SI Appendix*, Fig. S10 *A and B*). However, in the lungs of pneumonitis patients, RYK expression was markedly reduced in stromal cells, even though it was still high in epithelial cells of the airway and alveoli (*SI Appendix*, Fig. S10 *A and B*). We also examined CCL2 expression in those lungs. While CCL2 expression was specifically detected in immune cells in the lungs of healthy controls, it was significantly increased in stromal cells of pneumonitis patients (Fig. 4*I* and *SI Appendix*, Fig. S10*C*). These results are consistent with our mouse data, further indicating that in the lung, RYK restricts the immune response, including inflammatory cell recruitment.
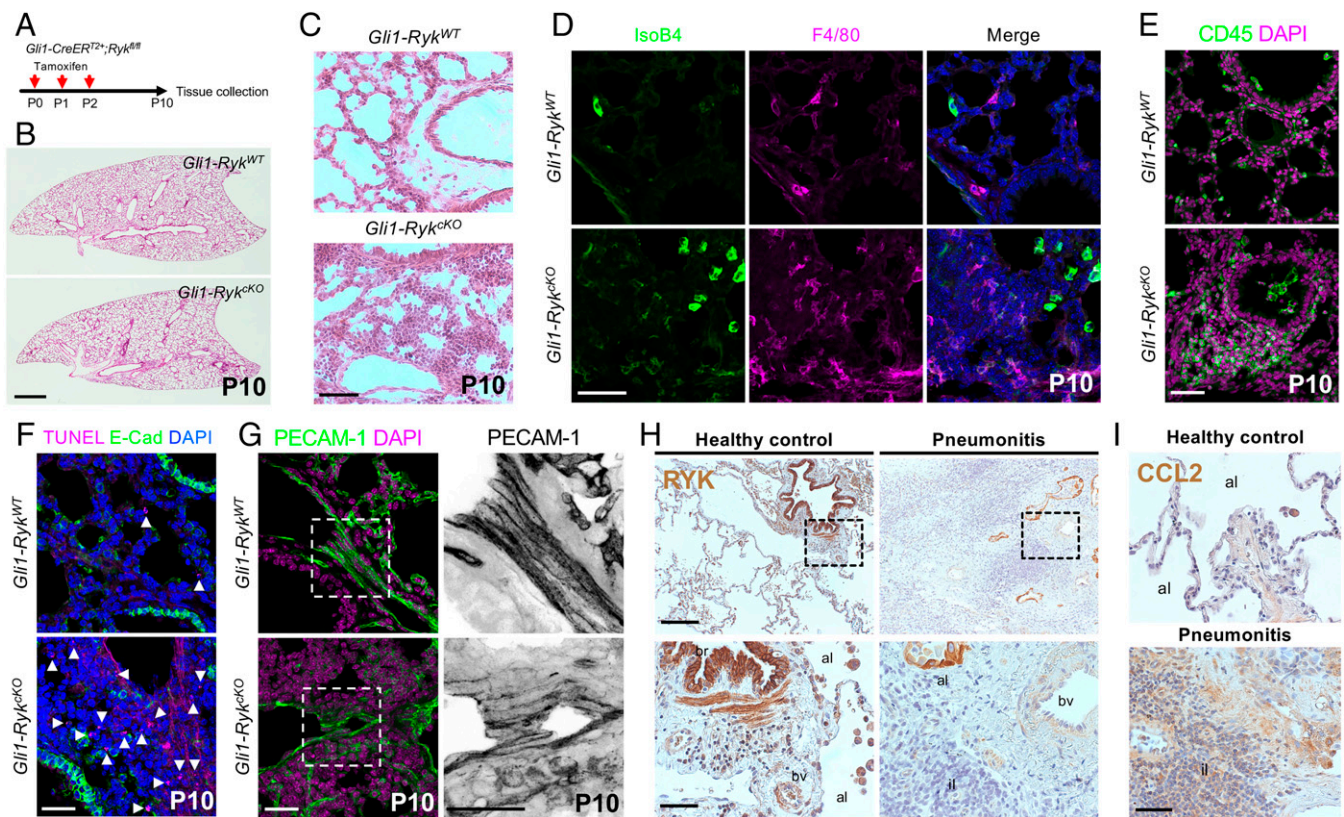
Fig. 4. RYK acts as a survival factor and antiinflammatory modulator during lung maturation and homeostasis. (*A*) Diagram indicating the time points of tamoxifen injections and tissue collection for the early postnatal *Gli1-Ryk^cKO* mice. (*B*) H&E staining of P10 *Gli1-Ryk^WT* (*n* = 6) and *Gli1-Ryk^cKO* (*n* = 6) lung sections. (*C*) High magnification of H&E-stained P10 *Gli1-Ryk^WT* (*n* = 6) and *Gli1-Ryk^cKO* (*n* = 6) lung sections. (*D*) IsoB4 staining (immune cells) and F4/80 immunostaining (alveolar and interstitial macrophages) in P10 *Gli1-Ryk^WT* (*n* = 6) and *Gli1-Ryk^cKO* (*n* = 6) lung sections. (*E*) Immunostaining for CD45 (hematopoietic cells) in P10 *Gli1-Ryk^WT* (*n* = 6) and *Gli1-Ryk^cKO* (*n* = 6) lung sections. (*F*) TUNEL staining and E-cadherin immunostaining in P10 *Gli1-Ryk^WT* (*n* = 6) and *Gli1-Ryk^cKO* (*n* = 6) lung sections. Arrowheads point to TUNEL-positive cells. (*G*) Immunostaining for PECAM-1 in P10 *Gli1-Ryk^WT* (*n* = 6) and *Gli1-Ryk^cKO* (*n* = 6) lung sections. High-magnification image of the areas in the dashed boxes is shown on the *Right*. (*H*) Immunostaining for RYK in the lungs of healthy controls (*n* = 5) and pneumonitis patients (*n* = 10). High-magnification image of the areas in the dashed boxes is shown on the *Bottom*. (*I*) Immunostaining for CCL2 in the lungs of healthy controls and pneumonitis patients. Abbreviations: al, alveoli; br, bronchiole; bv, blood vessel; and il, inflammatory lesion. (Scale bars: 1 mm for *B*; 200 μm for *H*, *Top*; 50 μm for *H*, *Bottom*, and *I*; and 30 μm for *D*, *F*, and *G*.)

Discussion

Here, we identify a role for RYK in the lung mesenchyme during lung development and maturation, as well as during homeostasis. In mesenchyme-specific *Ryk*-deficient lungs, inflammatory cells accumulate in airway lumens, alveolar spaces, and lung parenchyma, a phenotype accompanied by increased mesenchymal cell death and defective vessel integrity. We show that RYK inhibits proapoptotic and inflammatory genes in part through NF-κB. At later stages, encompassing lung maturation and homeostasis, RYK continues to promote mesenchymal cell survival and to dampen the immune response.

Abnormal inflammatory responses accompanied by infiltration of activated immune cells and release of proinflammatory mediators are observed in patients with inflammatory lung diseases such as COPD, IPF, asthma, as well as pneumonia (3, 4). WNT signaling plays a key role in both acute and chronic inflammation, and dysregulation of WNT/β-catenin signaling has been linked with the pathogenesis of these diseases (10, 11, 26). RYK, a coreceptor for WNT ligands, has been shown to participate in β-catenin–dependent and –independent signaling in a cell- and tissue-specific manner (12, 13, 27). In the present study, we found that, through dysregulation of β-catenin–dependent signaling, loss of *Ryk* function in the mouse lung mesenchyme leads to severe inflammation accompanied by overproduction of inflammatory cytokines, a process that is regulated by NF-κB signaling.

As WNT/β-catenin activation inhibits NF-κB signaling (22), our data support a model where WNT/RYK signaling constitutively inhibits the activation of NF-κB signaling, thereby repressing the expression and release of inflammatory cytokines from the lung mesenchyme.

Recently, a role for RYK in endothelial cells has been reported. *RYK* knockdown in human coronary artery endothelial cells in culture prevents WNT-5A–induced hyperpermeability, which occurs through cytoskeleton remodeling (17). In contrast, our in vivo data suggest that *Ryk* deficiency in lung mesenchymal cells, but not lung endothelial cells, is sufficient to cause defects in endothelial cell junctions and vessel permeability/integrity. It has previously been reported that *Ryk* is expressed in the bone marrow and that its expression is regulated during hematopoietic development and maturation (28). In addition, *Ryk* deficiency in hematopoietic stem cells (HSCs) from the fetal liver can reduce HSC self-renewal and lead to proliferation-induced apoptosis (29). We found that mice with myeloid lineage-specific *Ryk* deletion (*Lyz2-Ryk^cKO*) display no obvious inflammatory phenotypes in the lung, suggesting that RYK does not participate in myeloid cell proliferation and maturation in a cell-autonomous manner.

In the present study, the *Ryk* N-ethyl-N-nitrosourea (ENU) mutant mice (*Ryk^SL/SL*) and the *Dermo1-Ryk^cKO* mice, which express Cre recombinase in lung mesenchymal cells, all exhibit severe inflammation as well as developmental defects, including

lung hypoplasia and leaky blood vessels. In contrast, when we activated CreERT2 in $Gli1$-Ryk^{cKO} mice between P0 and P2 to conditionally delete Ryk in lung mesenchymal cells after birth, we observed lung inflammation and leaky blood vessels without obvious lung hypoplasia. The weaker phenotype in Gli-Ryk^{cKO} mice compared with both the $Ryk^{SL/SL}$ and the $Dermo1$-Ryk^{cKO} mice may be due to the fairly restricted vs. broader domain of Cre expression in $Gli1$-$CreER^{T2}$ and $Dermo1$-Cre mice, respectively. These observations, together with our results from the knockdown of Ryk in NIH 3T3 fibroblasts, indicate that the inflammation phenotype derives directly, or indirectly, from a cell-autonomous defect in lung mesenchymal cells. Nevertheless, we cannot exclude the possibility that the increased immune response is in part due to developmental defects, such as growth retardation.

The stimulation of WNT/β-catenin signaling leads to the up-regulation of antiapoptotic factors in hepatocytes (30). Activated WNT/β-catenin signaling inhibits apoptosis during development and tissue repair, as well as during tumorigenesis (31, 32). Moreover, WNT/β-catenin signaling has been shown to suppress the apoptosis of IPF myofibroblasts (7, 33). We found that Ryk deficiency leads to the increased expression of proapototic genes in mesenchymal cells, increased interstitial cell death, vessel permeability defects, and excessive immune cell recruitment and local proliferation. Inhibition of Caspase activity can attenuate the inflammation phenotype in Ryk mutant mice, possibly in part by reducing NF-κB phosphorylation. Overall, these results suggest that the increased expression of inflammatory cytokines observed in Ryk mutants is due to both direct and indirect effects, including signals released by dying cells.

Recently, severe acute respiratory syndrome coronavirus 2 (SARS-CoV-2)/coronavirus disease 19 (COVID-19) has been declared a pandemic. SARS-CoV-2 can, not only activate antiviral immune responses, but also cause uncontrolled inflammatory responses characterized by a cytokine storm (34, 35). Relevant to these processes, the mouse models in the present study recapitulate features of inflammatory lung diseases characterized by combined disruption of endothelial cell barrier function and excess immune responses.

In conclusion, we propose that during lung development and homeostasis, WNT signaling, through RYK, β-catenin, and NF-κB, plays an important role in safeguarding the lung mesenchyme against cell death and an exacerbated immune response, including increased inflammatory cytokine production and inflammatory cell recruitment and accumulation. This signaling axis could represent an important therapeutic target against inflammatory lung diseases, such as pneumonia and COPD.

Materials and Methods

All animal care and experimental procedures in this study were approved by the local animal ethics committee at the Regierungspräsidium Darmstadt, Hessen, Germany. Human pneumonitis lung samples and healthy control lungs were provided by the Universities of Giessen and Marburg Lung Center Biobank, which is a member of the Deutsches Zentrum für Lungenforschung (DZL) Platform Biobanking. The study protocol was approved by the ethics committee of the Justus Liebig University School of Medicine (no. 58/2015), and informed consent was obtained in written form from each patient. All human studies were performed in adherence to the relevant ethical guidelines.

For the transcriptome analysis, total RNA was isolated from P0 lungs of three $Dermo1$-Ryk^{WT} and three $Dermo1$-Ryk^{cKO} mice. For immune cell phenotyping, cells were obtained from P4 $Dermo1$-Ryk^{WT} and $Dermo1$-Ryk^{cKO} lungs.

The materials and methods used in this study are described in detail in *SI Appendix, Materials and Methods*.

Data Availability. The RNA-Sequencing dataset produced in this study (36) is available in the National Center for Biotechnology Information (NCBI) Gene Expression Omnibus (GEO) database at https://www.ncbi.nlm.nih.gov/geo/query/acc.cgi?acc=GSE141974.

Author affiliations: aDepartment of Developmental Genetics, Max Planck Institute for Heart and Lung Research, 61231 Bad Nauheim, Germany; bCardiopulmonary Institute, Max Planck Institute for Heart and Lung Research, 61231 Bad Nauheim, Germany; cMember of the German Center for Lung Research, Partner Site Universities of Giessen and Marburg Lung Center, 35392 Giessen, Germany; dSoonchunhyang Institute of Medi-Bio Science, Soonchunhyang University, 31151 Cheonan-si, Republic of Korea; eDepartment of Integrated Biomedical Science, Soonchunhyang University, 31151 Cheonan-si, Republic of Korea; fFlow Cytometry Facility, Max Planck Institute for Heart and Lung Research, 61231 Bad Nauheim, Germany; gInstitute for Oral Science, Matsumoto Dental University, 399-0781 Shiojiri, Japan; hBioinformatics and Deep Sequencing Platform, Max Planck Institute for Heart and Lung Research, 61231 Bad Nauheim, Germany; and iDZL (Deutsches Zentrum für Lungenforschung) Biobanking Platform, Universities of Giessen and Marburg Lung Center, 35392 Giessen, Germany

1. H. Alkhouri, W. J. Poppinga, N. P. Tania, A. Ammit, M. Schuliga, Regulation of pulmonary inflammation by mesenchymal cells. *Pulm. Pharmacol. Ther.* **29**, 156–165 (2014).
2. W. Broekman et al., Mesenchymal stromal cells: A novel therapy for the treatment of chronic obstructive pulmonary disease? *Thorax* **73**, 565–574 (2018).
3. E. P. Schmidt, R. M. Tuder, Role of apoptosis in amplifying inflammatory responses in lung diseases. *J. Cell Death* **3**, 41–53 (2010).
4. B. D. Levy, C. N. Serhan, Resolution of acute inflammation in the lung. *Annu. Rev. Physiol.* **76**, 467–492 (2014).
5. L. Zitvogel, O. Kepp, G. Kroemer, Decoding cell death signals in inflammation and immunity. *Cell* **140**, 798–804 (2010).
6. D. Wallach, T. B. Kang, A. Kovalenko, Concepts of tissue injury and cell death in inflammation: A historical perspective. *Nat. Rev. Immunol.* **14**, 51–59 (2014).
7. M. Sauler, I. S. Bazan, P. J. Lee, Cell death in the lung: The apoptosis-necroptosis axis. *Annu. Rev. Physiol.* **81**, 375–402 (2019).
8. M. Zhang, J. Shi, Y. Huang, L. Lai, Expression of canonical WNT/β-CATENIN signaling components in the developing human lung. *BMC Dev. Biol.* **12**, 21 (2012).
9. C. Ota, H. A. Baarsma, D. E. Wagner, A. Hilgendorff, M. Königshoff, Linking bronchopulmonary dysplasia to adult chronic lung diseases: Role of WNT signaling. *Mol. Cell Pediatr.* **3**, 34 (2016).
10. M. Hussain et al., Wnt/β-catenin signaling links embryonic lung development and asthmatic airway remodeling. *Biochim. Biophys. Acta Mol. Basis Dis.* **1863**, 3226–3242 (2017).
11. M. Königshoff, O. Eickelberg, WNT signaling in lung disease: A failure or a regeneration signal? *Am. J. Respir. Cell Mol. Biol.* **42**, 21–31 (2010).
12. J. Green, R. Nusse, R. van Amerongen, The role of Ryk and Ror receptor tyrosine kinases in Wnt signal transduction. *Cold Spring Harb. Perspect. Biol.* **6**, 6 (2014).
13. J. P. Roy, M. M. Halford, S. A. Stacker, The biochemistry, signalling and disease relevance of RYK and other WNT-binding receptor tyrosine kinases. *Growth Factors* **36**, 15–40 (2018).
14. H. T. Kim et al., WNT/RYK signaling restricts goblet cell differentiation during lung development and repair. *Proc. Natl. Acad. Sci. U.S.A.* **116**, 25697–25706 (2019).
15. E. R. Hollis II et al., Ryk controls remapping of motor cortex during functional recovery after spinal cord injury. *Nat. Neurosci.* **19**, 697–705 (2016).
16. S. Sarin et al., Role for Wnt signaling in retinal neuropil development: Analysis via RNA-Seq and in vivo somatic CRISPR mutagenesis. *Neuron* **98**, 109–126.e8 (2018).
17. T. Skaria, E. Bachli, G. Schoedon, Wnt5A/Ryk signaling critically affects barrier function in human vascular endothelial cells. *Cell Adhes. Migr.* **11**, 24–38 (2017).
18. C. E. Green, A. M. Turner, The role of the endothelium in asthma and chronic obstructive pulmonary disease (COPD). *Respir. Res.* **18**, 20 (2017).
19. P. Lertkiatmongkol, D. Liao, H. Mei, Y. Hu, P. J. Newman, Endothelial functions of platelet/endothelial cell adhesion molecule-1 (CD31). *Curr. Opin. Hematol.* **23**, 253–259 (2016).
20. M. M. Halford et al., Ryk-deficient mice exhibit craniofacial defects associated with perturbed Eph receptor crosstalk. *Nat. Genet.* **25**, 414–418 (2000).
21. K. McArthur, B. T. Kile, Apoptotic caspases: Multiple or mistaken identities? *Trends Cell Biol.* **28**, 475–493 (2018).
22. B. Ma, M. O. Hottiger, Crosstalk between Wnt/β-Catenin and NF-κB signaling pathway during inflammation. *Front. Immunol.* **7**, 378 (2016).

23. Q. Zhang, M. J. Lenardo, D. Baltimore, 30 years of NF-κB: A blossoming of relevance to human pathobiology. *Cell* **168**, 37–57 (2017).
24. A. J. Hoogendijk, S. H. Diks, T. van der Poll, M. P. Peppelenbosch, C. W. Wieland, Kinase activity profiling of pneumococcal pneumonia. *PLoS One* **6**, e18519 (2011).
25. W. Dai *et al.*, Blockade of Wnt/β-Catenin pathway aggravated silica-induced lung inflammation through Tregs regulation on Th immune responses. *Mediators Inflamm.* **2016**, 6235614 (2016).
26. W. J. Chae, A. L. M. Bothwell, Canonical and non-canonical Wnt signaling in immune cells. *Trends Immunol.* **39**, 830–847 (2018).
27. M. M. Halford, M. L. Macheda, S. A. Stacker, "The RYK receptor family" in *Receptor Tyrosine Kinases: Family and Subfamilies*, D. L. Wheeler, Y. Yarden, Eds. (Humana, 2015), pp. 685–741.
28. D. K. Simoneaux *et al.*, The receptor tyrosine kinase-related gene (Ryk) demonstrates lineage and stage-specific expression in hematopoietic cells. *J. Immunol.* **154**, 1157–1166 (1995).
29. F. Famili *et al.*, The non-canonical Wnt receptor Ryk regulates hematopoietic stem cell repopulation in part by controlling proliferation and apoptosis. *Cell Death Dis.* **7**, e2479 (2016).
30. F. Götschel *et al.*, Inhibition of GSK3 differentially modulates NF-kappaB, CREB, AP-1 and beta-catenin signaling in hepatocytes, but fails to promote TNF-alpha-induced apoptosis. *Exp. Cell Res.* **314**, 1351–1366 (2008).
31. S. Chen *et al.*, Wnt-1 signaling inhibits apoptosis by activating beta-catenin/T cell factor-mediated transcription. *J. Cell Biol.* **152**, 87–96 (2001).
32. N. Pećina-Slaus, Wnt signal transduction pathway and apoptosis: A review. *Cancer Cell Int.* **10**, 22 (2010).
33. W. Chang *et al.*, SPARC suppresses apoptosis of idiopathic pulmonary fibrosis fibroblasts through constitutive activation of beta-catenin. *J. Biol. Chem.* **285**, 8196–8206 (2010).
34. L. A. Teuwen, V. Geldhof, A. Pasut, P. Carmeliet, COVID-19: The vasculature unleashed. *Nat. Rev. Immunol.* **20**, 389–391 (2020).
35. C. Matacic, Blood vessel injury may spur disease's fatal second phase. *Science* **368**, 1039–1040 (2020).
36. H. T. Kim, S. Guenther, D. Y. R. Stainier. Transcriptome of P0 Dermo1-RykWT and Dermo1-RykcKO lungs. Gene Expression Omnibus (GEO) database. https://www.ncbi.nlm.nih.gov/geo/query/acc.cgi?acc=GSE141974. Deposited 13 December 2019.